ARL-TR-10414 ● Sep 2026

Mechanical Evaluation of Additive Manufacturing Polymers for Cold Weather Environments, Including a Dual-Material Thermoplastic Elastomer Filament

by Ryan M. Dunn, Kyle D. Olchewsky, Nikhil Patil, Jay H. Park, and Eric D. Wetzel

NOTICES

Disclaimers

ARL-TR-10414 ● SEP 2026

Mechanical Evaluation of Additive Manufacturing Polymers for Cold Weather Environments, Including a Dual-Material Thermoplastic Elastomer Filament

Ryan M. Dunn and Eric D. Wetzel
DEVCOM Army Research Laboratory

Kyle D. Olchewsky
SURVICE Engineering

Nikhil Patil and Jay H. Park
University of Massachusetts

REPORT DOCUMENTATION PAGE

1. REPORT DATE	2. REPORT TYPE	3. DATES COVERED	
		START DATE	END DATE
September 2026	Technical Report	1 October 2024	30 July 2026

4. TITLE AND SUBTITLE
Mechanical Evaluation of Additive Manufacturing Polymers for Cold Weather Environments, Including a Dual-Material Thermoplastic Elastomer Filament

5a. CONTRACT NUMBER	5b. GRANT NUMBER	5c. PROGRAM ELEMENT NUMBER
W911NF-19-2-0100		
5d. PROJECT NUMBER	**5e. TASK NUMBER**	**5f. WORK UNIT NUMBER**

6. AUTHOR(S)
Ryan M. Dunn, Kyle D. Olchewsky, Nikhil Patil, Jay H. Park, and Eric D. Wetzel

7. PERFORMING ORGANIZATION NAME(S) AND ADDRESS(ES)	8. PERFORMING ORGANIZATION REPORT NUMBER
DEVCOM Army Research Laboratory ATTN: FCDD- RLA-MD Aberdeen Proving Ground, MD 21005	ARL-TR-10414

9. SPONSORING/MONITORING AGENCY NAME(S) AND ADDRESS(ES)	10. SPONSOR/MONITOR'S ACRONYM(S)	11. SPONSOR/MONITOR'S REPORT NUMBER(S)

12. DISTRIBUTION/AVAILABILITY STATEMENT
DISTRIBUTION STATEMENT A. Approved for public release: distribution unlimited.

13. SUPPLEMENTARY NOTES
ORCIDs: Kyle D. Olchewsky, 0009-0009-9116-8776; Eric D. Wetzel, 0000-0002-0176-3702

14. ABSTRACT
Izod testing is used to compare room temperature and cold temperature (–40 °C) impact strength for 3D-printed thermoplastic parts. Comparisons are made for in-plane (y-direction) and interlayer (z-direction) part orientations. The results show that all parts exhibit lower strength under cold conditions and for z-direction interfaces. However, acrylonitrile butadiene styrene (ABS) and Nylon 3D-printed parts show the lowest toughness values, while parts printed using polycarbonate and polybutylene terephthalate (PCPBT) and a dual material ABS+ thermoplastic elastomer (TPE) core-shell filament both show remarkably high toughness under cold conditions. In fact, these materials provide cold in-plane impact strengths that are nearly 10 times higher than a benchmark injection-molded Nylon part. PCPBT shows clear evidence of ductility even under cold conditions. Additional experiments attempt to apply a loop elastica test on 3D-printing filaments to characterize intrinsic cold toughness.

15. SUBJECT TERMS
fused filament fabrication, fused deposition modeling, impact strength, toughness, cold, polycarbonate and polybutylene terephthalate, PCPBT, acrylonitrile polybutadiene styrene, thermoplastic elastomer, ABS+TPE, Nylon, elastica loop, Sciences of Extreme Materials

16. SECURITY CLASSIFICATION OF:			17. LIMITATION OF ABSTRACT	18. NUMBER OF PAGES
a. REPORT	b. ABSTRACT	C. THIS PAGE		
UNCLASSIFIED	UNCLASSIFIED	UNCLASSIFIED	UU	33

19a. NAME OF RESPONSIBLE PERSON	19b. PHONE NUMBER *(Include area code)*
Eric D. Wetzel	(520) 691-5002

STANDARD FORM 298 (REV. 5/2020)
Prescribed by ANSI Std. Z39.18

Contents

List of Figures

List of Tables

1. Introduction

The U.S. Army is required to perform operations in all environments, including cold climates. Polymers are known to embrittle at cold temperatures,[1–5] which makes plastic parts particularly challenging to engineer to provide strength and toughness for cold climates.

3D printing has emerged as a key technology for rapid, distributed, and point-of-need production of thermoplastic parts. Fused filament fabrication (FFF) is the most commonly practiced form of 3D printing, in which a thermoplastic filament is melted and extruded from a computer-controlled gantry to produce a solid object. The object is fabricated in a layer-wise manner, with each layer comprising many individual extruded traces of thermoplastic. These parts tend to be weaker and more brittle than conventional, injection-molded parts, especially when considering mechanical behavior between layers.[6,7] Interlayer mechanical strength is typically 5–10 times lower than the in-plane strength of these parts. Under cold conditions, these interfaces are expected to be even weaker.[8,9]

The U.S. Army Combat Capabilities Development Command (DEVCOM) Army Research Laboratory (ARL) recently demonstrated dual-material (DM) filaments composed of two thermoplastics in a regular arrangement in the filament cross section.[10–12] Most commonly, the filament cross section has a core and a shell, where the core can be round or star-shaped. Combining two thermoplastics into a single filament provides new opportunities for processing and properties of 3D-printed parts. Prior studies showed that parts printed with a polycarbonate (PC) core and an acrylonitrile butadiene styrene (ABS) core can be annealed after printing to achieve high z-direction strength.[10–12] Other studies have shown that a rigid ABS core can be combined with an elastomeric shell to print soft, deformable parts, or to produce parts with strongly anisotropic mechanical behavior.[13,14]

In this study, we perform mechanical testing on FFF, 3D-printed thermoplastics under room temperature (RT) and cold (–40 °C) conditions. Filament feedstocks include conventional off-the-shelf filaments, as well as a novel DM filament comprising a thermoplastic elastomer (TPE) shell and a rigid, ABS core. Both in-plane and interlayer mechanical properties are tested and benchmarked relative to an injection-molded Nylon. Izod testing is used for mechanical characterization, due to its sensitivity to brittleness and relevance to low-velocity impacts that are commonly experienced under military environments.

2. Experimental

2.1 Materials

The following five materials were evaluated via Izod testing:

1) **Nylatron:** Solid blocks of injection-molded Nylatron NSM (Boedeker Plastics; Shiner, Texas) were cut and machined into shape for Izod impact testing. Nylatron NSM is semi-crystalline Nylon 6 manufactured by Mitsubishi Chemical Group (Reading, Pennsylvania) and has a melting temperature of approximately 215 °C. Nylatron is marketed as self-lubricating, with a proprietary solid lubricant additive. Manufacturer data lists a minimum service temperature of –30 °C, due to reduced impact strength at lower temperatures.
2) **Nylon:** 1.75-mm-diameter clear Taulman Bridge Nylon (formerly Taulman 3D, now Xtellar; Philadelphia, Pennsylvania) was purchased from the distributor Matterhackers (York, Pennsylvania). Taulman Bridge Nylon is semi-crystalline and has a glass transition temperature (T_g) of 52 °C.
3) **ABS:** Two types of ABS were used for fracture studies. For *z*-direction fracture testing, 1.75-mm-diameter naturally colored MG94 ABS filament was purchased from Essentium (Essentium, Inc.; Pflugerville, Texas). MG94 ABS polymer is produced as CYCOLAC MG94 from SABIC (Exton, Pennsylvania). MG94 has a T_g of approximately 105 °C. The 1.78-mm-diameter red Stratasys (Eden Prairie, Minnesota) M30 ABS, purchased from the distributor Computer Aided Technology Inc. (GoEngineer; Ambler, Pennsylvania), was used for *y*-direction ABS fracture specimens. ABS M30 properties are known to be very similar to those of MG94 ABS,[10] such that their mechanical behaviors can be considered identical. This filament is slightly larger than standard 1.75-mm-diameter-sized filaments but still works on nearly all commercial printers that accept 1.75-mm-diameter filaments. Extrusion multiplier adjustments are made to compensate for the larger diameter.
4) **PCPBT:** PCPBT refers to a blend of amorphous PC and semi-crystalline polybutylene terephthalate (PBT). Black 1.75-mm-diameter PCPBT filament was purchased from IC3D (Hillard, Ohio). The PCPBT used in the manufacturing of this filament is Xenoy Resin 1102 (SABIC; Exton, Pennsylvania). The exact glass transition of this blend is not available in technical data sheets and is

expected to be sensitive to varying degrees of crystallinity from thermal history.

5) **ABS+TPE:** A custom DM filament consisting of an ABS core and TPE shell was manufactured using a DM extrusion technique, as described previously.[13,14] The ABS is MG94, and the TPE is thermoplastic silicone vulcanate (TPSiV) 4200 with a durometer of 75A (DuPont; Wilmington, Delaware). The TPE is a silicone vulcanate, which refers to a blend of thermoplastic elastomer with a crosslinked silicone phase. These TPEs exhibit excellent toughness and solvent resistance. The equipment used to manufacture this custom filament produces elliptical filament, which is undesirable when trying to maintain a precise extrusion amount. The minor diameter of this filament was as low as 1.4 mm while the major diameters were as large as 1.8 mm. Special care is needed to calibrate extrusion multipliers when printing with elliptical filament. The filament used had an ABS content of 62% volume (Figure 1).

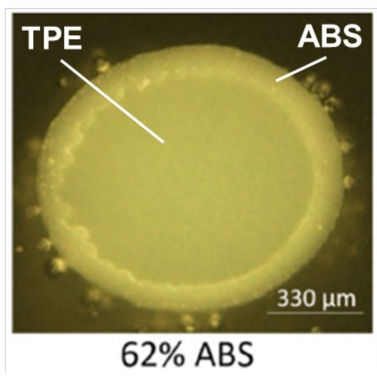

Figure 1. Cross-sectional micrograph of the ABS+TPE filament.

The following materials were only evaluated for the loop elastica method, all received as 1.75-mm filament for 3D printing, except for the ABS M30 at 1.79-mm diameter.

PLA: Polylactic acid (PLA) from Prusament (Prusa Research; Czech Republic) is a commonly used rigid polymer for 3D printing.

ABS M30: Red Stratasys ABS M30 (as described earlier).

TPU-M: Matterhackers (York, Pennsylvania) thermoplastic urethane generically labeled “TPU.”

TPE-M: Matterhackers (York, Pennsylvania) generically labeled “TPE.”

TPU-C: TC Poly (Atlanta, Georgia) Ice9 Rigid is a carbon-loaded Nylon filament marketed as a thermally conductive, structural thermoplastic.

Nylon-C: TC Poly (Atlanta, Georgia) Ice9 Flex is a carbon-loaded TPU filament marketed as a thermally conductive, semi-flexible thermoplastic.

2.2 Sample Preparation

Molded Nylatron was machined into 12.7- × 12.7- × 63-mm rectangular prisms from a large block of material for Izod testing.

All MG94 and ABS+TPE samples were prepared on a Prusa MK3+ (Prusa Research; Czech Republic) with a print speed of 40 mm/s, bed temperature of 75 °C, line width of 0.5 mm, and layer height of 0.2 mm. The nozzle temperature was 240 °C for ABS, and 210 °C for ABS+TPE. The models were generated with PrusaSlicer version 2.6, a fork of Slic3r tailored for the Prusa model printers. All PCPBT, ABS M30, and Taulman Nylon samples were prepared on the AON M2 (Montreal, Quebec, Canada) with a print speed of 40 mm/s, line width of 0.5 mm, and a layer height of 0.2 mm. The nozzle temperature was 240 °C for ABS M30, 250 °C for Taulman Nylon, and 260 °C for PCBPT. The bed temperature was 110 °C for ABS M30, 45 °C for Taulman Nylon, and 90 °C for PCPBT. AON M2 print files were prepared using Simplify3D 5.2 (Simplify3D; Cincinnati, Ohio). The AON M2 has no part fans although the chamber experiences forced convection from fans circulating outside air to maintain the chamber at room temperature; chamber heating was not used in this study as chamber heating is expected to affect interlaminar strength.

Interlaminar strength is highly dependent on the fractional fill of the sample, referred to in this study as part density. Simply specifying an infill percentage of 100% in the slicer will not ensure high part density if the extrusion is not properly calibrated. For ABS and ABS+TPE samples, part density was carefully tuned according to the following procedure. A 20- × 20- × 20-mm cube was printed. If the outer dimensions of the resulting print were not accurate to within ±0.1 mm, an XY size compensation was set to ensure dimensional accuracy. The mass of the part was then divided by the actual measured volume of the sample, and the volume of the printed model. If the resulting density was below 95%, the extrusion modifier was increased and a new sample was characterized. This process was repeated until at least 95% density was achieved. Reaching 100% density is generally not practical without overextruding to an extent that leads to surface roughness and dimensional inaccuracies.

3D-printed Izod samples are referred to as either *z*-oriented or *y*-oriented (Figure 2). The *y*-oriented samples are printed horizontally and notched such that fracture surface is primarily in the *x*-*z* plane. The *z*-oriented samples are printed vertically and notched such that the resulting fracture surface is in the *x*-*y* plane.

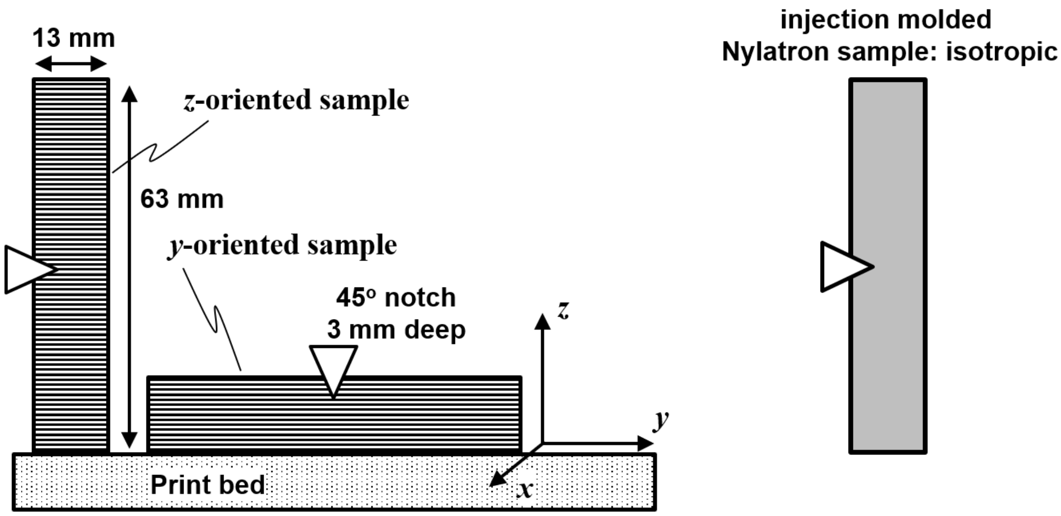

Figure 2. Schematics for *z*-direction and *y*-direction print orientations, and isotropic configuration, for Izod test samples.

A number of infill patterns were implemented. For *y*-direction samples, the ABS, PCPBT, and ABS+TPE samples were sliced with "aligned" infill such that all traces are parallel to each other equivalent to an "all perimeter" slicing configuration or a "rectilinear" infill with every layer set to a 0° orientation. For Nylon, a 0–90 rectilinear infill, with two perimeters, was used. For MG94 ABS, a 0–90 rectilinear infill with four perimeters was used. In the *z*-direction, all samples used a 0–90 infill, with two perimeters for Nylon and PCPBT samples, and four perimeters for MG94 ABS and ABS+TPE samples.

Some *z*-direction ABS and ABS+TPE samples were subject to a thermal annealing step after printing, but before notching. ABS samples were annealed at 135 °C for 72 h. ABS+TPE samples were annealed at 80 °C for 72 h.

2.3 DSC Testing

Differential scanning calorimetry (DSC) on the TPSiV material was performed using a Mettler Toledo 3+ (Columbus, Ohio) DSC. The sample was ramped at 10 °C/min from –90 to 210 °C in a nitrogen gas environment.

2.4 Cold Conditioning

All Izod samples tested below room temperature were placed in a Platinous environmental chamber (ESPEC North America; Hudsonville, Michigan) at the appropriate set point for at least 12 h. After conditioning, the samples were placed in an insulated container along with a metal block that had also been cold-conditioned. The metal block provided additional thermal mass to keep the environment in the container cold. The samples were removed from the container one at a time for testing with the lid returned immediately after sample extraction. To minimize thermal conduction at the test region, the samples were not handled near the pre-crack. Care was made to ensure samples were not exposed to room temperature for more than 2 min before they were tested.

2.5 Izod Impact Testing

Notched Izod impact testing was used to evaluate the impact resistance of sample parts at all test temperatures. Izod samples were notched using a Qualitest 45° 0.25-mm-radius broach and Qualitest motorized notch machine (Qualitest Advanced Testing Technologies; Fort Lauderdale, Florida) to ensure a final notch geometry consistent with ASTM D256.[15] Annealed samples were notched after annealing to ensure a sharp crack tip. All *y*-direction samples were notched parallel to the *x*-axis (as shown in Figure 2), except for the ABS+TPE samples, which were notched parallel to the *y*-axis.

Izod impact testing was performed in accordance with ASTM D256[15] and carried out on a Dynatup POE 2000 impact tester (Instron; Norwood, MA). For *z*-direction samples, a 2.71 N-m (2 ft-lb) pendulum was used, released from a 90° horizontal position, at a height of 0.62 m. For *y*-orientation and injection-molded samples, a 25.6 N-m (19 ft-lb) pendulum was used to ensure full sample fracture. Energy loss was calculated using either force-displacement data from a tup accelerometer or using visual change of height measurements from image analysis of recorded impact videos. (The accelerometer failed partway through the study, necessitating a switch to video measurements). After each test, the samples were collected and the width and depth of the fracture surfaces were recorded for impact toughness calculations.

2.6 Optical Microscopy

Optical images of fracture surfaces were obtained with a VHX-7000 microscope (KEYENCE; Osaka, Japan) at 20× magnification.

2.7 Elastica Loop Testing

An elastica loop test was evaluated as a potential method for rapid screening of printer filaments for cold conditions. The elastica loop test is a method of obtaining the tensile properties of fibers by measuring the smallest loop the filament can form before fracturing. A relatively flexible fiber will be able to form a small loop, while a very brittle fiber of comparable fiber diameter would fracture or kink while attempting to form a small loop.[16,17] The mean radius (r_m) of the smallest possible loop is used to establish a critical compressive strain given by

$$\varepsilon_{cr} = d/2r_m \,, \tag{1}$$

where d is the diameter of the filament.

A schematic of the test is shown in Figure 3a. To perform the test, the fiber was pinned between two clear plates separated by a gap slightly larger than twice the filament diameter. Two sheets of PC were held apart with bolts, using metal washers as spacers to ensure a gap of 3.5 mm for purposes of testing 1.75-mm filament. Two guiding rings formed an entrance and exit path through which both ends of the filament could be pulled simultaneously. To conduct a test, the two ends of the filament were pulled manually and the loop formed by the filament was filmed as it reduced in diameter. The test was concluded when the loop kinked or fractured. The last frame before failure of the video was extracted and used to measure r_m with the circle measurement tool in ImageJ (National Institutes of Health, Bethesda, Maryland). The outer dimensions of the PC plates were used as a reference for length scaling.

Filaments were tested at room temperature, and also at –40 °C. The test apparatus was sized to fit inside the Platinous cold chamber (Figure 3b). Filaments were mounted in the apparatus and exposed to –40 °C conditions for at least 1 h, at which point the freezer door was opened and the fiber was tested immediately. Black posterboard was used as a backdrop when contrast for filming with the filament is required.

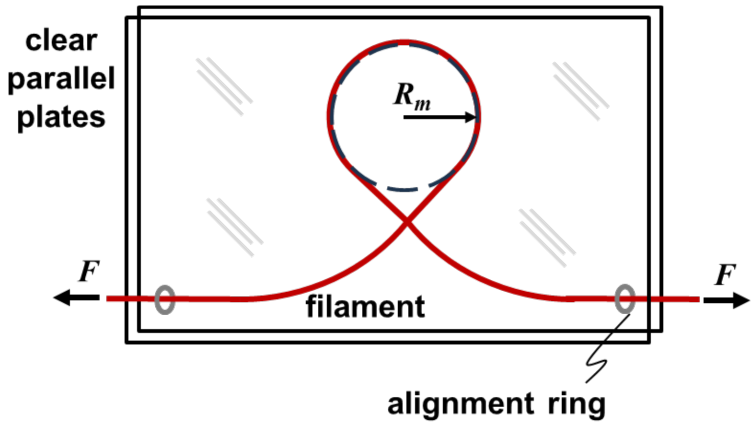

(a)

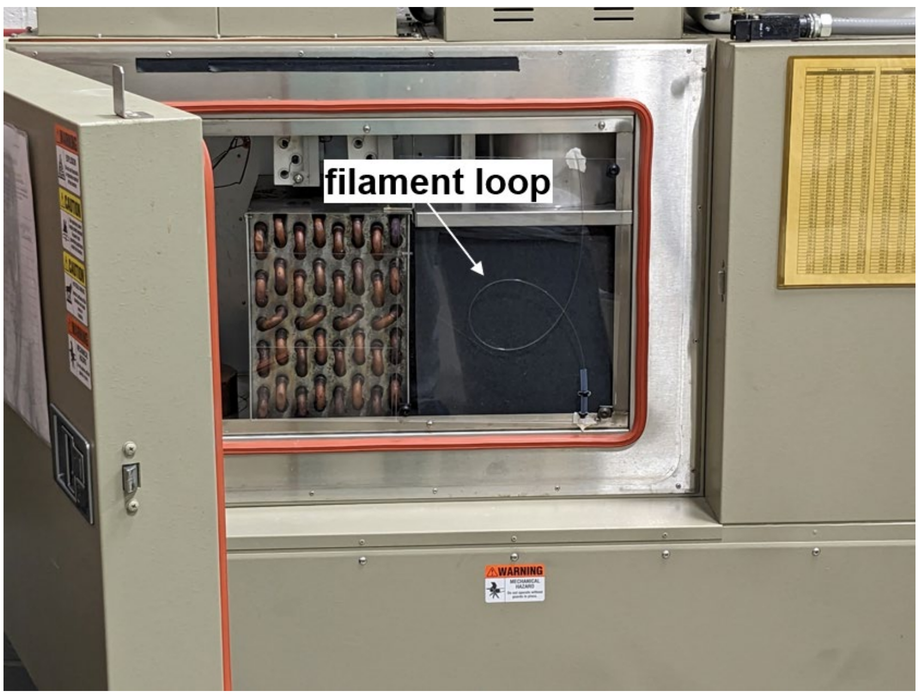

(b)

Figure 3. Elastica loop test (a) schematic and (b) setup in the cold conditioning chamber.

3. Results

3.1 DSC

Figure 4 shows the DSC results for the TPSiV material. The onset T_g, defined as the temperature of maximum tangent slope in the heat flow versus temperature response during heating from below T_g, is approximately –47 °C. This value is below the Army operating environment goal of –40 °C. However, the negative peak in the heat flow during heating is very close to –40 °C, suggesting that material transitions are still underway at that temperature; the peak has subsided by –30 °C.

Taken together, these results suggest that the TPSiV material should remain rubbery down to –30 °C, but may begin to undergo a transition to a glassier material as the cold condition of –40 °C is reached.

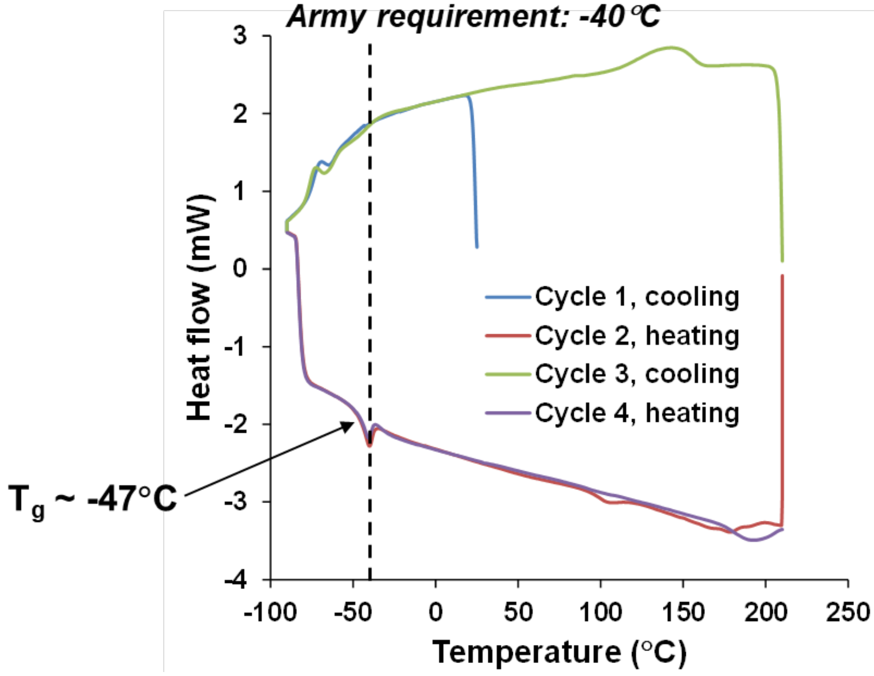

Figure 4. DSC results for the TPSiV (TPE) material.

3.2 Room Temperature Performance

Table 1 summarizes the RT Izod impact results, which are also plotted in Figure 5 for *y*-oriented samples, and Figure 6 for *z*-oriented samples. The *y*-oriented samples induce fracture cohesively within extrusion traces, so they are most representative of intrinsic material performance. For this reason, the printed Nylon impact strength is comparable to that of the injection-molded Nylatron. The printed ABS sample exhibits 2–3 times higher impact strength than the Nylon materials, perhaps due to the known toughening effect of the butadiene inclusions in ABS. The PCPBT and ABS+TPE materials show remarkable impact toughnesses, over 10 times higher than the Nylon and Nylatron materials.

Table 1. RT Izod impact response.

Orientation	Material	Annealed?	Temp. (°C)	Impact strength (kJ/m²)	Impact strength (J/m)
Molded	Nylatron	N	23	4.31	43.1
y	Nylon	N	23	3.61	36.1
y	ABS	N	23	11.37	113.7
y	PCPBT	N	23	48.71	487.1
y	ABS+TPE	N	23	50.61	542.1
z	ABS	N	23	0.48	4.8
z	PCPBT	N	23	1.97	19.7
z	Nylon	N	23	2.56	25.6
z	ABS+TPE	N	23	5.91	59.1
z	ABS	Y	23	1.90	19.0
z	ABS+TPE	Y	23	5.76	57.6

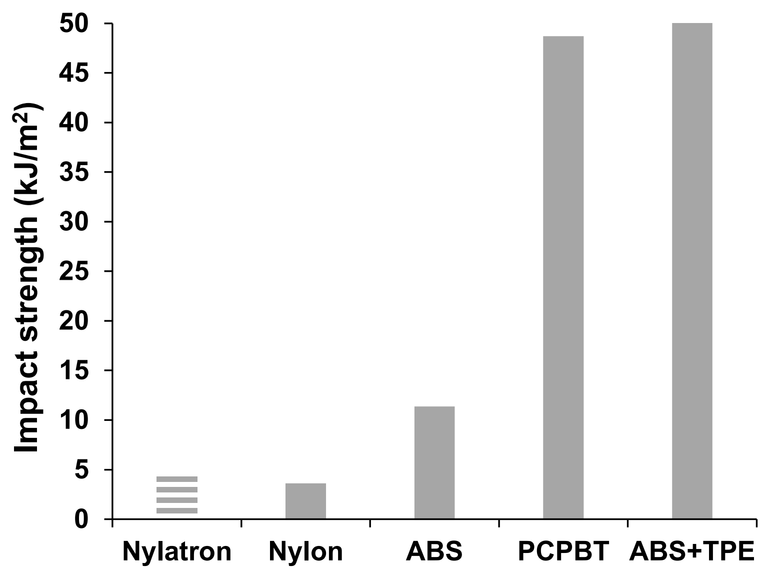

Figure 5. RT behavior for molded Nylatron and 3D-printed *y*-oriented materials.

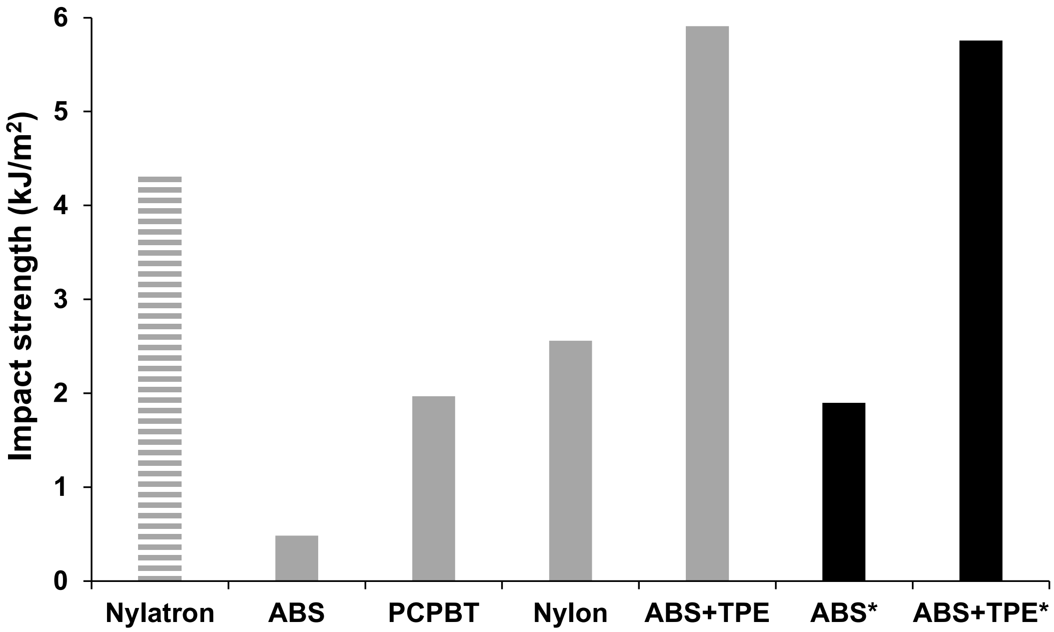

Figure 6. RT behavior for molded Nylatron and 3D-printed *z*-oriented materials, including materials subject to a thermal post-anneal (indicated by *).

The *z*-oriented Izod impact strength data (Figure 6) quantifies the behavior of failure between print layers and is therefore lower than the *y*-oriented Izod data. The ABS impact strength is the lowest, over 20 times lower than ABS in the *y*-orientation. PCPBT also shows a dramatic loss in impact strength, exhibiting over 20 times reduction compared with *y*-oriented samples. Nylon's *z*-direction and *y*-direction fracture strength are comparable, perhaps because Nylon is semi-crystalline and would be expected to have a lower viscosity melt interface during printing compared with amorphous polymers like ABS. The highest *z*-direction fracture toughness value is for ABS+TPE, likely due to a combination of the softness of the elastomer phase as well as the low T_g of the TPE phase that suggests higher polymer mobility during printing. The fracture toughness of the ABS+TPE is also higher than that of the injection-molded Nylatron material at room temperature.

Annealing the ABS specimens led to a 4 times increase in *z*-direction Izod impact strength, less than the 10 times increase in annealed Izod impact strength previously observed for ABS.[11] Annealing the ABS+TPE sample did not increase its *z*-direction fracture strength.

3.3 Cold Temperature Performance

Table 2 summarizes the cold temperature Izod impact results, which are also plotted in Figure 7 for *y*-oriented samples, and Figure 8 for *z*-oriented samples. Under cold conditions, the Nylatron impact strength decreases by 33% relative to room temperature, consistent with general observations of polymer embrittlement with decreasing temperature. Nylon and ABS show cold *y*-direction impact strength values comparable to Nylatron, with ABS showing a 74% loss in strength from room temperature. PCPBT and ABS+TPE again show remarkably high *y*-direction strength under cold conditions, over 10 times higher than molded Nylatron, although at 30%–50% lower performance compared with the same materials at room temperature. In fact, the cold impact strength for the PCPBT and ABS+TPE samples are over 5 times higher than the Nylatron strength at RT.

Table 2. Cold (–40 °C) Izod impact response.

Orientation	Material	Annealed?	Temp. (°C)	Impact strength (kJ/m²)	Impact strength (J/m)	RT to cold strength change
Molded	Nylatron	N	–40	2.9	29.0	–33%
y	Nylon	N	–40	2.71	27.1	–25%
y	ABS	N	–40	3.00	30.0	–74%
y	PCPBT	N	–40	32.88	328.8	–32%
y	ABS+TPE	N	–40	27.39	295.3	–46%
z	ABS	N	–40	0.51	5.1	6%
z	PCPBT	N	–40	1.41	14.1	–28%
z	Nylon	N	–40	2.21	22.1	–14%
z	ABS+TPE	N	–40	2.22	22.2	–62%
z	ABS	Y	–40	1.25	12.5	–34%
z	ABS+TPE	Y	–40	1.70	17.0	–70%

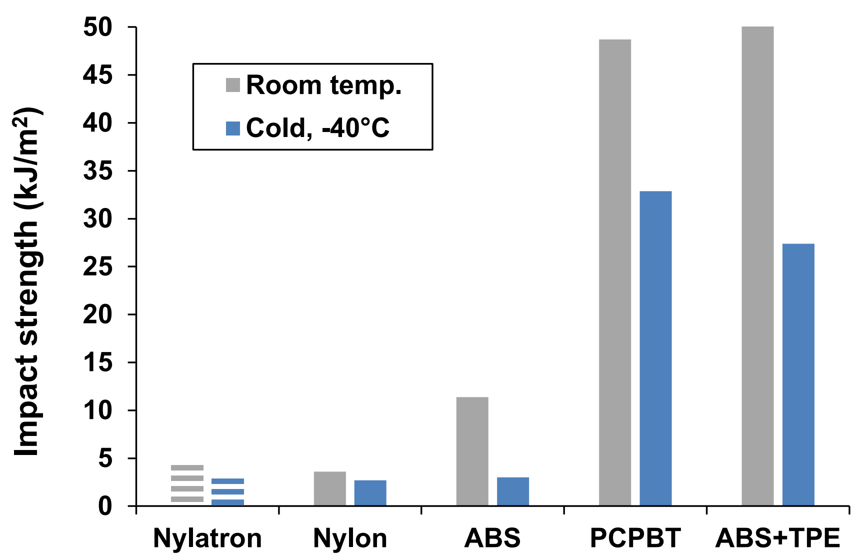

Figure 7. Comparison of RT and cold behavior for molded Nylatron and 3D-printed *y*-oriented materials.

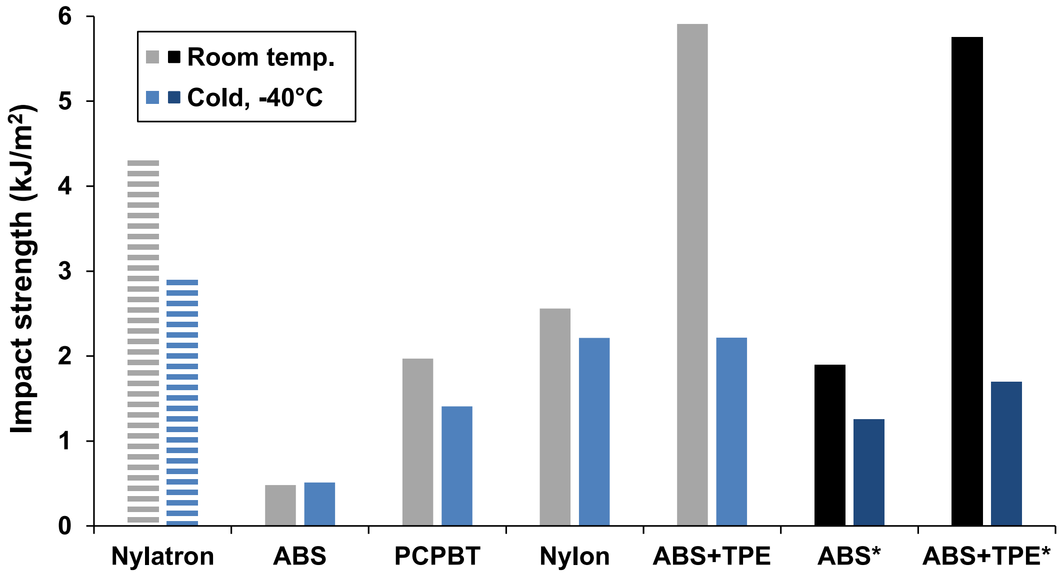

Figure 8. Comparison of RT and cold behavior for molded Nylatron and 3D-printed *z*-oriented materials, including materials subjected to a thermal post-anneal (indicated by *).

In the *z*-direction, all impact strengths are much lower compared with *y*-direction strengths. For ABS, PCPBT, and Nylon, the *z*-direction impact strengths are comparable at RT and under cold conditions, suggesting that cold embrittlement does not further weaken the interfaces. ABS+TPE, however, shows a significant 62% loss in toughness from RT to cold conditions. Despite this embrittlement, the ABS+TPE and PCPBT samples are still exhibiting the highest fracture toughness under cold conditions for the 3D-printed specimens. The Nylatron sample, which is isotropic, shows higher cold strength than the *z*-direction ABS+TPE and PCPBT samples.

Annealing ABS results in roughly a doubling of its fracture strength under cold conditions, although it is still lower than the cold fracture toughness of Nylatron. Interestingly, annealing the ABS+TPE samples results in lower impact strength compared with unannealed samples.

Table 3 and Figure 9 show Izod impact strength data for *z*-direction ABS+TPE samples at temperatures of RT, 0, –20, and –40 °C. A clear and steady downward trend is evident. Given that the TPE has a T_g of around –40 °C (Figure 4), the TPE component in these test specimens should remain rubbery under all tested conditions. Therefore, it seems likely that the drop in toughness is likely due to embrittlement of the ABS core, which comprises 62% of the composite volume. Other possible mechanisms are described in Section 4.

Table 3. Izod impact response of 3D-printed ABS+TPE specimens (*z*-orientation) as a function of temperature.

Orientation	Material	Annealed?	Temp. (°C)	Impact strength (kJ/m²)
Cast	ABS+TPE	N	23	5.91
z	ABS+TPE	N	0	5.80
z	ABS+TPE	N	–20	4.46
z	ABS+TPE	N	–40	2.22

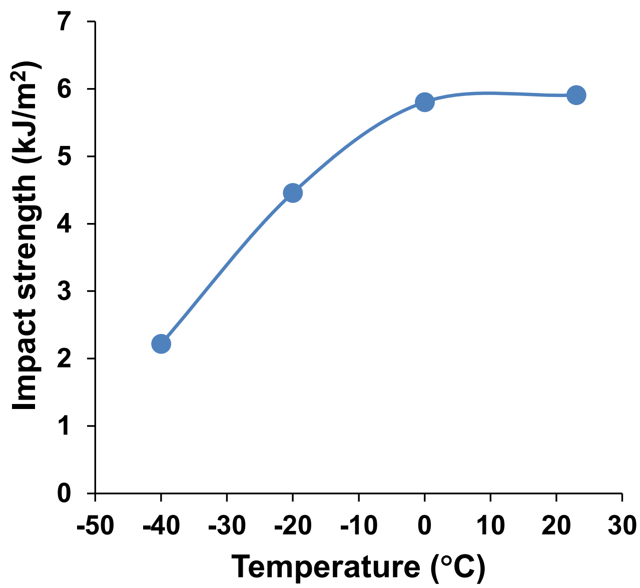

Figure 9. Izod impact response of 3D-printed ABS+TPE specimens (*z*-orientation) as a function of temperature.

3.4 Fracture Surfaces

Room temperature and cold fracture surfaces for Nylatron are given in Figure 10. Both fracture images are nearly identical and show a single violent fracture event indicative of brittle fracture. These images are consistent with the impact strength data, which showed low impact strength under both RT and cold conditions.

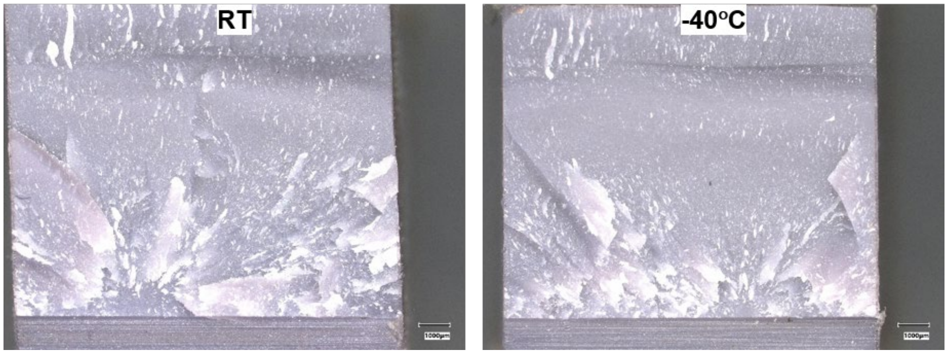

Figure 10. Fracture surfaces for Nylatron.

Fracture surfaces for the 3D-printed Nylon samples are shown in Figure 11. These samples appear to be underfilled, with significant gaps between extrusion traces. Under both orientations and temperatures, similar fracture strength values were measured (ranging from 2.21–3.61 kJ/m^2). The fracture surfaces at RT and under cold conditions are also similar in appearance. Comparing *y*-direction and *z*-direction fractures, both show clean and flat interfaces. This result is somewhat surprising, as most 3D-printed parts will show high strength and toughness in the *y*-direction, because *y*-direction failure requires tensile failure of extruded polymer traces, whereas *z*-direction failure only requires a failure between layers. The isotropy in mechanical properties could suggest that the polymer has a low melt viscosity and therefore is able to quickly form entangled interlayer bonding. Furthermore, the low melt viscosity could also imply a lower molecular weight, which would lead to the low fracture strengths observed in these experiments.

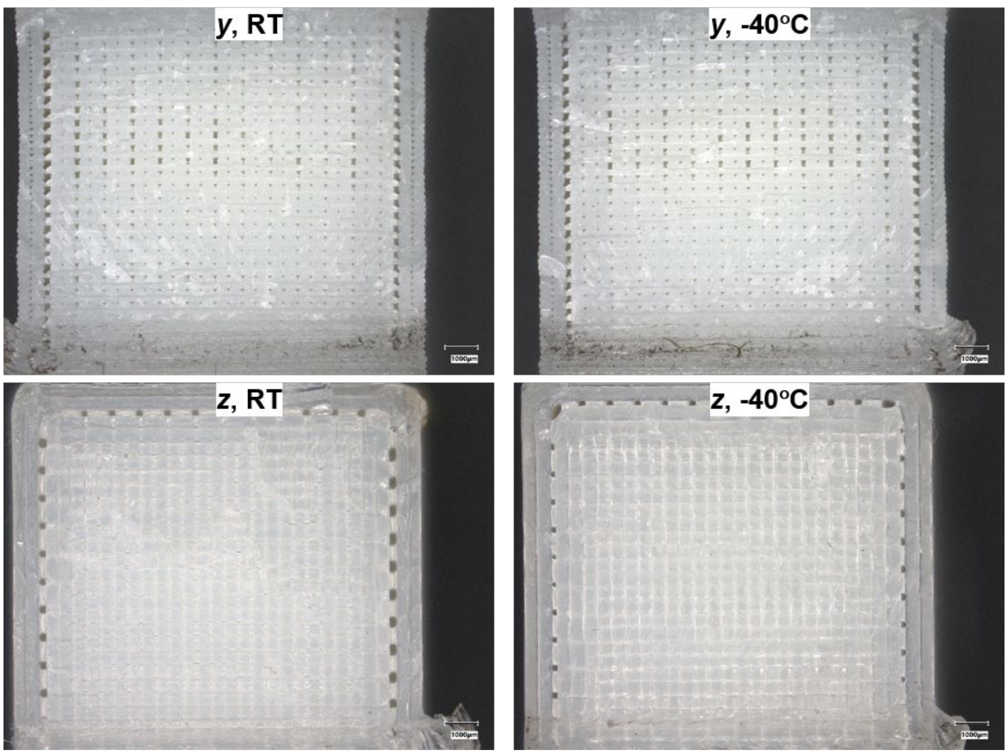

Figure 11. Fracture surfaces for Nylon.

ABS fracture surfaces are shown in Figure 12. For *y*-direction samples, the RT fracture surface is regular and shows some whitening, suggestive of a steady plastic failure. In contrast, the cold fracture surface suggests a more violent, brittle failure. In the *z*-direction, at RT the surface is smooth and appears to have failed along a single plane between print layers. Interestingly, at –40 °C, the failure surface crosses multiple layers, a behavior that is more typically associated with ductile failure. The annealed ABS samples exhibit less pronounced extrusion lines, and the cold-conditioned sample shows very little evidence of extrusion lines. These images suggest that annealing was effective at enabling flow across layer-to-layer interfaces, which is reflected in a 2–4 times increase in fracture strength, relative to unannealed ABS, for both RT and cold experiments.

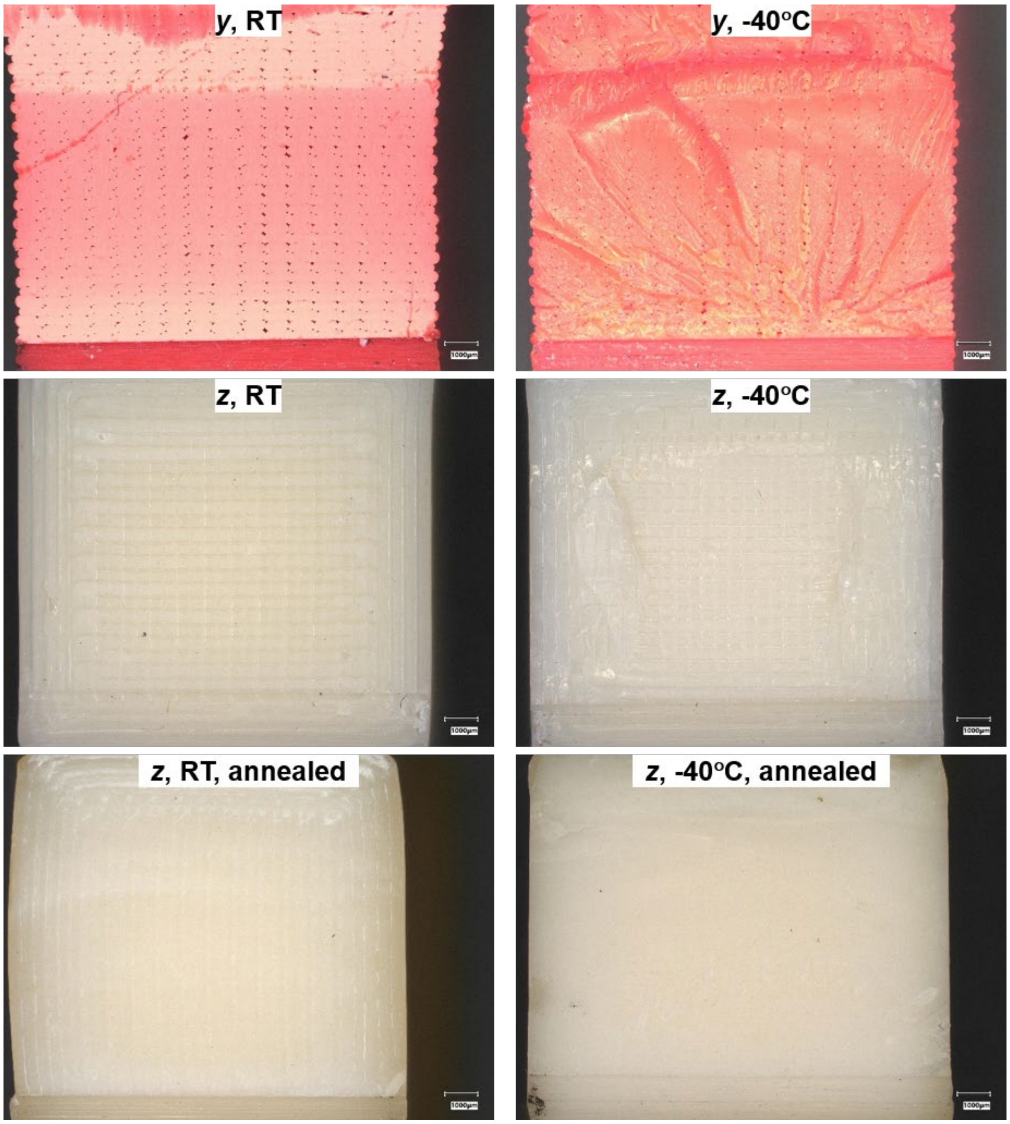

Figure 12. Fracture surfaces for ABS. The red (*y*-direction) specimens are M30 ABS; the white (*z*-direction) specimens are MG94 ABS.

For PCPBT fracture surfaces (Figure 13), the first observation for *y*-orientation fracture surfaces is the large apparent gaps between traces. These gaps are in part due to the usual gaps between traces. However, the gaps are exaggerated due to plastic deformation in the material. That is, during fracture, the *y*-oriented extrusion traces are stretched and neck down to a smaller diameter before breaking, resulting in the large apparent gaps between traces. This necking is observed across the full fracture surface at RT. Under cold impact, the region near the initiation crack exhibits necking, while the region away from the fracture surface exhibits fracture without necking. These images suggest a partial transition to brittle behavior at –40 °C. In the *z*-direction, some of this extrudate necking is evident at RT (although the necking occurs parallel to the traces), while under cold conditions there is little evidence of this necking behavior.

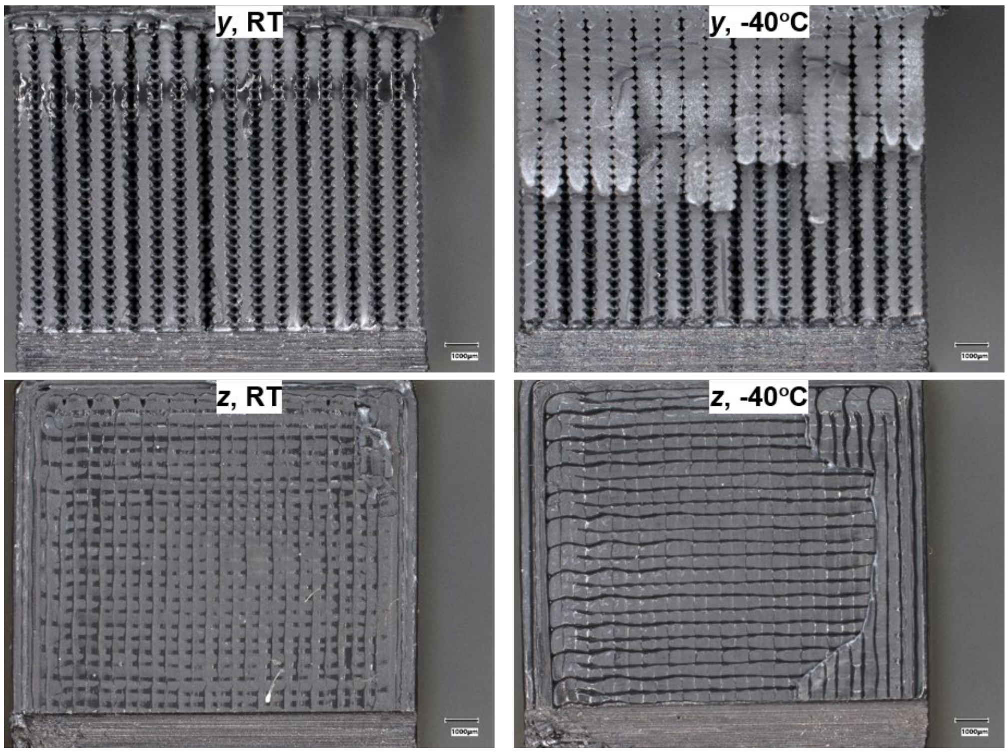

Figure 13. Fracture surfaces for PCPBT.

For the ABS+TPE sample, *y*-direction fracture surfaces are shown in Figure 14. At RT, a rough fracture surface indicative of high toughness is evident. Under cold conditions, the fracture surface is also very rough, but the appearance suggests a rapid and brittle failure event. The zoomed-in micrograph at the bottom of Figure 14 confirms that the ABS and TPE phases remain distinct in the printed specimen, and there is no evidence of failure at the interface between ABS and TPE.

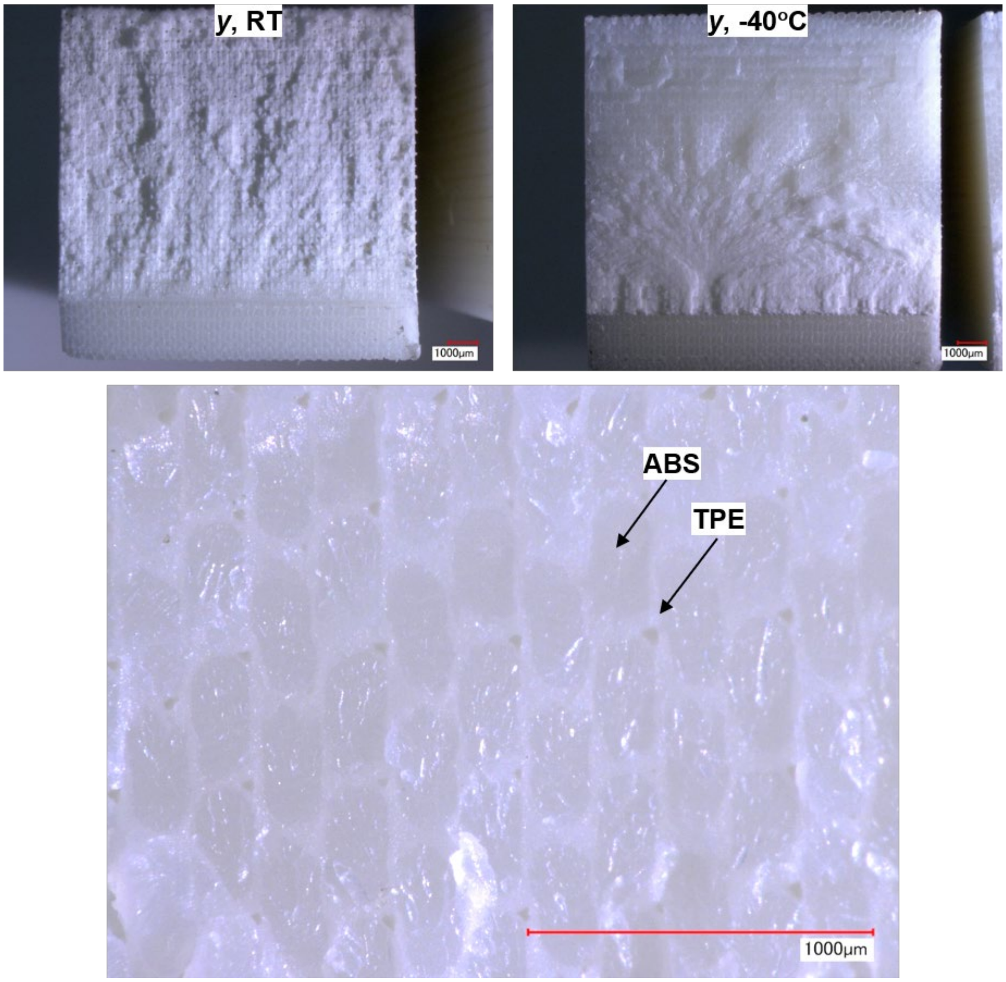

Figure 14. Fracture surfaces for ABS+TPE (*y*-direction). ABS and TPE phases are evident in the magnified image of the cold, *y*-direction fracture surface.

Z-oriented fracture surfaces for ABS+TPE are shown in Figure 15. All samples show multilayer fracture suggestive of tough behavior, rather than clean planar failure between two print layers. There is no obvious change in morphology from RT through –40 °C, even though the fracture strength steadily decreased with decreasing temperature (Figure 9). The annealed samples still show evidence of individual traces, although they might have softened slightly relative to the as-printed specimens.

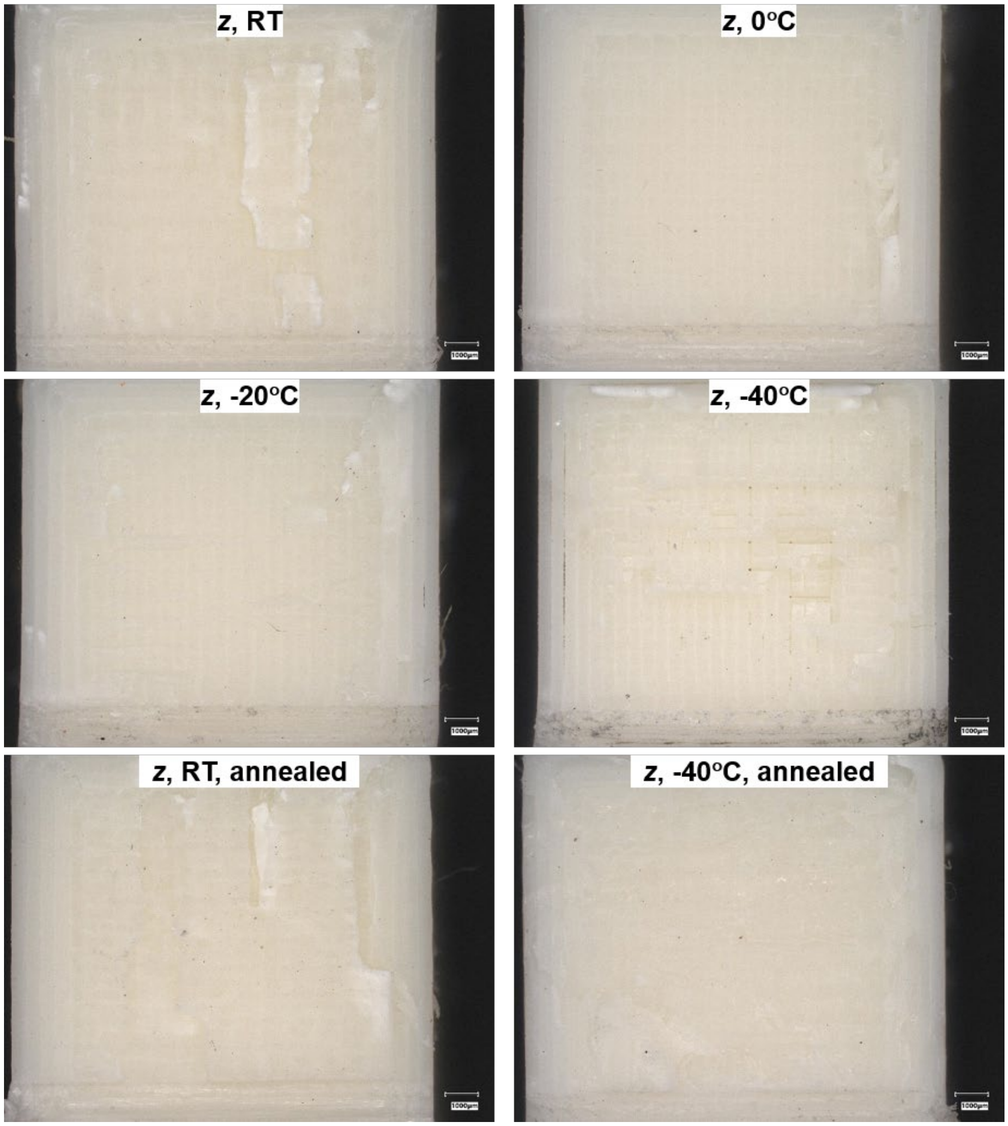

Figure 15. Fracture surfaces for ABS+TPE (*z*-direction).

3.5 Loop Elastica Results

Significant challenges limited the effectiveness of this test. Most notably, relatively flexible filaments like ABS and TPU are so flexible that they do not fracture in an obvious and measurable fashion (Figure 16, left side). For materials that do not fail, critical compressive strain cannot be calculated. Furthermore, pulling was performed by hand and thus the displacement rate was not precisely controlled. Further use of the elastica loop test would benefit from automated controlled rate testing if an accurate, quantitative critical compressive strain is desired.

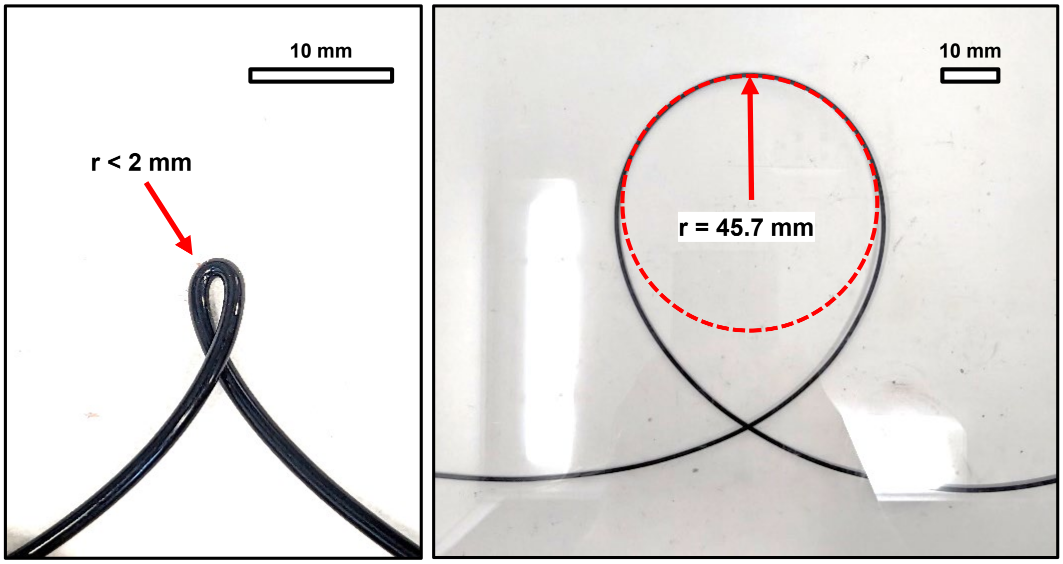

Figure 16. (Left) Unsuccessful elastica loop test of RT PCPBT. (Right) Elastica loop critical radius of Nylon-C immediately before failure.

Despite these challenges, some elastica loop data was collected. Of the materials tested, shown in Table 4, only PLA and Nylon-C (Figure 16, right side) were stiff enough to fail with measurable critical radii at RT. At –40 °C, all filaments except for TPU-M and TPE-M failed with a measurable radius. This data confirms the general trend of cold embrittlement. Ranking the materials for cold weather durability based on the magnitude of their critical strain at –40 °C, the data suggests that Nylon-C is the least suitable. This finding is reasonable, as the high carbon loading in Nylon-C makes it unusually brittle. PLA exhibits the next lowest critical strain, lower than ABS, consistent with the fact that ABS is known to be tougher than PLA at room temperature. The TPU-C shows a low critical compressive strain, likely due to the high loading of carbon particles. The TPU-M and TPU-E having unmeasurable critical strains, even at –40 °C, confirms that they are likely to be tough materials under cold conditions. The low critical strain of the PCPBT, lower than ABS, is very surprising given the extraordinary cold toughness of PCPBT (over 10 times higher Izod impact strength than ABS, Table 2).

Table 4. Elastica loop critical compressive strain results.

Material	Critical radius RT (mm)	Critical radius –40 °C (mm)	Filament diameter (mm)	Critical strain (ε_{cr}) RT (%)	Critical strain (ε_{cr}) –40 °C (%)
Nylon-C	45.7	132.1	1.75	40.1	0.03
PLA	5.7	16.2	1.75	4.95	0.22
TPU-C	. . .	6.1	1.75	. . .	0.57
PCPBT	. . .	5.0	1.76	. . .	0.70
ABS (M30)	. . .	4.2	1.78	. . .	0.85
TPU-M	. . .	. . .	1.75	. . .	. . .
TPE-M	. . .	. . .	1.74	. . .	. . .

4. Discussion

4.1 Intrinsic Toughness of PCPBT

One significant finding of this study is the truly remarkable toughness of PCPBT. The *y*-direction impact strength at room temperature, which is most representative of intrinsic material behavior, is over 4 times higher than ABS, normally considered one of the toughest engineering thermoplastics. Its fracture toughness is also nearly 10 times higher than the injection-molded Nylatron polymer, which is used in Army applications. Under cold conditions, the PCPBT sees some reduction in *y*-direction impact strength, but overall still provides 10 times more impact strength than ABS. Of note are the micrographs (Figure 13) showing extreme necking, rather than low-strain brittle fracture, under cold conditions for PCPBT. These images provide clear evidence of continued ductility under cold conditions. For all these reasons, PCPBT is clearly worthy of further investigation for Army 3D-printing applications. Additionally, a deeper investigation of the polymer physics of PCPBT during cold deformations would likely inspire new concepts for environmentally resilient polymers.

4.2 Performance of ABS+TPE Compared with Conventional Polymers

Like PCPBT, the ABS+TPE composite exhibits unusual intrinsic toughness. Under RT conditions, *y*-direction impact strength is equivalent to PCPBT, and over 10 times higher than the Nylatron toughness. This result is striking, given that the composition of this composite part is 62% ABS. Said differently, including 40% of the TPE into the ABS material leads to a 4 times increase in impact strength. Under cold conditions, the effect is even more extreme: ABS+TPE impact strength is nearly 10 times higher than both ABS alone and Nylatron. Mechanistically, the TPE phase is likely blunting cracks; the periodic ABS and TPE arrangement is steering and deflecting crack progression; and the high strain to failure of the TPE is bridging cracks and absorbing energy during crack progression. The micrographs show no indication of separation between the TPE and the ABS, suggesting good adhesion consistent with prior investigations.[13,14]

Compared with PCPBT, the ABS+TPE exhibits improved *z*-direction impact strength: at RT and under cold conditions, the ABS+TPE values are 3 times and 1.5 times better than PCPBT. The ABS+TPE *z*-direction properties are also comparable to the Nylatron impact strength values at RT and cold conditions. Therefore, this 3D-printed ABS+TPE material could be a reasonable substitute for Nylatron parts.

Annealing of ABS+TPE resulted in very little strength improvement. This behavior could be related to the low intrinsic strength of the TPE, which is only 12.1 MPa,[14] and is comparable to the *z*-direction strength for as-printed ABS. This intrinsic strength is much lower than, for example, ABS, whose tensile strength is closer to 43 MPa.[11] Therefore, even if the part has fully entangled TPE interfaces, the ultimate strength will be limited.

A further consideration is elastic stiffness, or Young's modulus, of these parts. Using rule of mixture estimates,[14] the *y*-direction and *z*-direction stiffness of the ABS+TPE specimens would be 1.6 and 0.12 GPa, respectively. In contrast, ABS and PCPBT have modulus values around 2.3–2.5 GPa, and Nylatron has a stiffness of 3.1. To some extent, the low *z*-direction stiffness can be managed via careful infill design.[13] However, the increased toughness of ABS+TPE is at the cost of decreased stiffness.

4.3 Potential DM Combinations

Additional material innovations are possible to create improved DM filaments for cold weather endurance. First, considering ABS+TPE, the effects of ABS volume fraction can be studied. It is possible that only a small fraction of TPE is needed to add toughness; for example, if 10% TPE provides sufficient impact strength, then the resulting stiffness of the ABS+TPE composite would be more similar to conventional ABS (rule of mixtures estimate is 2.3 GPa[14]). Another consideration is evaluating other elastomers, such as TPUs or other TPEs.

The core material could also be changed. There are hundreds of ABS grades available commercially, with vastly different morphologies that directly influence toughness[18] including under cold conditions. For example, a high-impact ABS with higher rubber content is likely to be tougher under cold conditions. ABS is also commonly blended with polycarbonate (PC-ABS), to create tough and stiff thermoplastics; this material would be worthy of consideration for a filament core. Polycarbonate copolymers[10] (such as Apec XT from Covestro) are also known to exhibit excellent cold weather toughness. Finally, the PCPBT material exhibited outstanding intrinsic cold toughness in the present study. It would be interesting to see how much better the toughness would become for a PCPBT-TPE composite.

An additional design exploration to address *z*-direction strength would be to place the soft/elastomeric phase in the filament core, and the rigid thermoplastic in the cladding. The advantage of this approach would be to increase the limiting tensile strength in the *z*-direction, as rigid thermoplastics will have a much higher intrinsic strength than soft TPEs or TPUs. The disadvantage of this approach is that there would be a continuous lattice of rigid polymer, which might lead to rapid and brittle crack propagation under cold conditions. The approach is worth testing, as the presence of elastomeric cores penetrating throughout a 3D rigid polymer might be enough to blunt and deflect cracks comparable to the use of spherical rubber inclusions in rubber-toughened polymers like ABS.

A further material pairing would be a PCPBT with a rigid, high strength core. For example, polyetheretherketone and polyetherketoneketone maintain high strength and toughness at low temperatures. Additionally, their high melting temperature (>300 °C) relative to the T_g of PCPBT (~130–150 °C) would allow printed parts to be annealed above the T_g of PCPBT and hopefully lead to further improvements in the *z*-direction toughness for PCPBT parts.

5. Conclusions

This study demonstrates that 3D-printed parts can provide cold toughness values significantly better than injection-molded thermoplastics. Both single material PCPBT filaments and DM ABS+TPE filaments are strong candidates for 3D printing parts for these cold condition applications. Results show that *z*-direction properties for 3D-printed parts remain significantly weaker than in-plane properties, highlighting an opportunity for further materials and manufacturing development to improve these properties. A further consideration is that time-temperature-superposition principles suggest that cold behavior correlates with high strain-rate behavior. Therefore, the PCPBT and ABS+TPE materials studied herein could be interesting candidates for polymer structures that require ductility under high rate-impact conditions.

6. References

1. Lu ML, Chiou KC, Chang FC. Effect of temperature on fracture toughness of PC/ABS based on J-integral and hysteresis energy methods. Journal of Applied Polymer Science. 1996;62(6):863–874.

2. Castellani L, Frassine R, Pavan A, Rink M. Rate and temperature dependence of fracture toughness in ABS resins in relation to dispersed-phase structure. Polymer. 1996;37(8):1329–1338.

3. Han Y, Lach R, Grellmann W. Effects of rubber content and temperature on ductile tearing stability in ABS materials. Die Angewandte Makromolekulare Chemie. 1999;270(1):5–12.

4. Han Y, Lach R, Grellmann W. Effects of rubber content and temperature on dynamic fracture toughness of ABS materials. Journal of Applied Polymer Science. 2000;75(13):1605–1614.

5. Han Y, Lach R, Grellmann W. Effects of rubber content and temperature on unstable fracture behavior in ABS materials with different particle sizes. Journal of Applied Polymer Science. 2001;79(1):9–20.

6. Cole DP, Riddick JC, Jaim HMI, Strawhecker KE, Zander NE. Interfacial mechanical behavior of 3D printed ABS. Journal of Applied Polymer Science. 2016;133(30):43671.

7. Hart KR, Wetzel ED. Fracture behavior of additively manufactured acrylonitrile butadiene styrene (ABS) materials. Engineering Fracture Mechanics. 2017;177:1–13.

8. Saenz F, Otarola C, Valladares K, Rojas J. Influence of 3D printing settings on mechanical properties of ABS at room temperature and 77 K. Additive Manufacturing. 2021;39:101841.

9. Weiss KP, Bagrets N, Lange C, Goldacker W, Wohlgemuth J. Thermal and mechanical properties of selected 3D printed thermoplastics in the cryogenic temperature regime. IOP Conference Series: Materials Science and Engineering. 2015;102(1):012022.

10. Pugatch M et al. Accelerated annealing of fused filament fabricated (FFF) thermoplastics via an improved core-shell filament. Scientific Reports. 2023;13(1):13538.

11. Koker B et al. Enhanced interlayer strength and thermal stability via dual material filament for material extrusion additive manufacturing. Additive Manufacturing. 2022;55:102807.

12. Hart KR, Dunn RM, Wetzel ED. Tough, additively manufactured structures fabricated with dual-thermoplastic filaments. Advanced Engineering Materials. 2020;22(4):1901184.

13. Patil NA et al. Controlled mechanical anisotropy in 3D-printed, thermoplastic elastomeric composites. Macromolecular Materials and Engineering. 2026;331(1):e00285. https://doi.org/10.1002/mame.202500285

14. Patil NA et al. Additive manufacturing of thermoplastic elastomer structures using dual material core-shell filaments. Additive Manufacturing. 2024;82:104044. https://doi.org/10.1016/j.addma.2024.104044

15. ASTM D256. Standard test methods for determining the Izod pendulum impact resistance of plastics. ASTM International; 2023.

16. Leal AA, Deitzel JM, Gillespie JW Jr. Compressive strength analysis for high performance fibers with different modulus in tension and compression. Journal of Composite Materials. 2009;43(6):661–674.

17. Fukuda H, Yakushiji M, Wada A. A loop test to measure the strength of monofilaments used for advanced composites. Advanced Composite Materials. 1999;8(3):281–291.

18. Lee J, Patil NA, Park JH. Correlating microstructural and rheological variations in acrylonitrile-butadiene-styrene (ABS) with interlayer bond formation in material extrusion additive manufacturing. Additive Manufacturing. 2024;96:104553.

List of Symbols, Abbreviations, and Acronyms

3D	Three-Dimensional
ABS	Acrylonitrile Butadiene Styrene
ARL	Army Research Laboratory
ASTM	American Society for Testing and Materials
DEVCOM	U.S. Army Combat Capabilities Development Command
DM	Dual Material
DSC	Differential Scanning Calorimetry
FFF	Fused Filament Fabrication
PBT	Polybutylene Terephthalate
PC	Polycarbonate
PCPBT	Polycarbonate and Polybutylene Terephthalate
PLA	Polylactic Acid
r_m	Mean Radius
RT	Room Temperature
T_g	Glass Transition Temperature
TPE	Thermoplastic Elastomer
TPSiV	Thermoplastic Silicone Vulcanate
TPU	Thermoplastic Urethane

1 (PDF)	DEFENSE TECHNICAL INFORMATION CTR DTIC OCA
1 (PDF)	DEVCOM ARL FCDD RLB CB TECH LIB